Back to Session Subjects

ALUMINIUM FOAM: A NEW MATERIAL FOR HELICOPTERS

Ottmar Schultz, Rudolf Schindler

Eurocopter Deutschland GmbH, Munich, Germany

Abstract

Currently, the powder-metallurgy and the melt-metallurgy processes for producing aluminium foam have reached the most advanced stage of maturity. Both manufacturing methods as well as the aluminium foams that can be achieved thereby are presented and compared.

To this end, specimens of both types of aluminium foam are fatigue-tested with a selected specimen geometry. The cyclical loading on the specimens was effected uniaxially so that the stress alternated between the equally large plus (tensile) and minus (compressive) values. The stress amplitude was then varied from one specimen to the next and the test procedure was able to establish the greatest loading endured "infinitely often" ($N \geq 10^7$) without fracture. These data were used to determine the fatigue strength for both types of aluminium foam tested, and S-N curves were calculated using Weibull's method. Hysteresis was also measured for different loadings to provide information on the specific fatigue behaviour of the two types of aluminium foam. Fracture surfaces of representative fatigue-tested specimens were recorded and compared to complete the analysis.

Resulting from these findings concerning the behaviour and properties of the aluminium foams investigated and the associated manufacturing methods, the service step of the EC135 was finally selected as being a promising demonstrator. This "simpler" component of the secondary structure of the helicopter should serve to demonstrate the potential of an integral aluminium-foam construction as is made possible by the powder-metallurgical process, in order to be able to evaluate the applicability of aluminium foam to more complex secondary structural components of a helicopter.

1 Introduction

In search of light materials with specific high stiffnesses, metal foams represent an interesting possibility. In contrast to plastic foams, metal foams exhibit major advantages with respect to strength, temperature resistance and environmental compatibility. Highly porous metal foams also broaden the spectrum of properties as regards energy absorption, sound and heat insulation as well as direction-independent behaviour when loaded.

In the past few years, the quality of aluminium foam has been enhanced considerably due to recent process developments. Of the diverse possible processes for making aluminium foam, the melt and powder-metallurgical processes have reached the most advanced stage of maturity. Furthermore, different types of aluminium foam have been partly characterised, and the properties achieved have been presented at international conferences such as, for instance, "MetFoam '99 – Bremen, D" and "Metal Foam Symposium '00 – Vienna, A". Further, aluminium foam, taking into consideration the manufacturing process, opens up a whole host of new possibilities for users, especially with respect to the reduction of tooling and production costs in view of the relatively low component weight. For these reasons it appears expedient to evaluate aluminium foam with respect to applications in secondary helicopter structures. If the material properties, quality and availability are right, in the final resort the factors determining the selection of material and production

process for helicopter components are costs and weight.

The individual components and materials of a helicopter in operation are subjected to continuously changing and repeated loads. Even if the maximum loads occurring are often lower – frequently even very much lower – than the static strength values of the materials used, the fatigue strength indeed constitutes a major material property which must be known in order to design the helicopter reliably for continuous operation. For this reason it is indispensable to gather experience with respect to the fatigue behaviour, fatigue strength and the failure of aluminium foam and to build up fundamental know-how. Only then is it possible, naturally taking into account manufacturing-specific possibilities as well as further complementary specific material characteristics, to evaluate possible future applications for aluminium foam in an extremely dynamically loaded environment as is represented, for instance, by a helicopter.

Taking into account the know-how about the material properties of different aluminium foams and the related manufacturing methods, the service step of the EC135 was selected as being a very promising demonstrator for 3d near net-shape components. The present service step of the EC135 is a complex honeycomb sandwich design. It seemed to be possible to simplify the design of the present service step by using aluminium foam and the related manufacturing techniques but still fulfilling the main design criteria.

In the following, first of all the two processes currently at the most advanced stage of maturity for producing aluminium foam are presented, namely the powder- and the melt-metallurgical process. Further, the fatigue behaviour, the fatigue strength and the type of failure shall be analysed, compared and discussed for both types of aluminium foam. Finally, test results of a design approach based on an aluminium-foamed body will be presented for a first helicopter component, the service step of the EC135.

2 The Production of Aluminium Foam

Of the various possible processes for making aluminium foam, the melt- and powder-metallurgical methods have currently attained the most advanced stage of maturity. Aluminium-foam semi-finished products made using these two manufacturing methods were studied as regards their future application in a helicopter. Each of these two manufacturing processes covers a characteristic bandwidth of density, cell size and cell topology. The feature shared by both methods is that the aluminium foam that is produced has closed pores. Both production processes are presented in the following.

2.1 Powder-metallurgical Process

The powder-metallurgical method for producing aluminium foam is based on commercial powders of aluminium or aluminium alloys, which are mixed with small amounts of a likewise powdered foaming agent (e.g. titanium hydride) (see Fig.1).

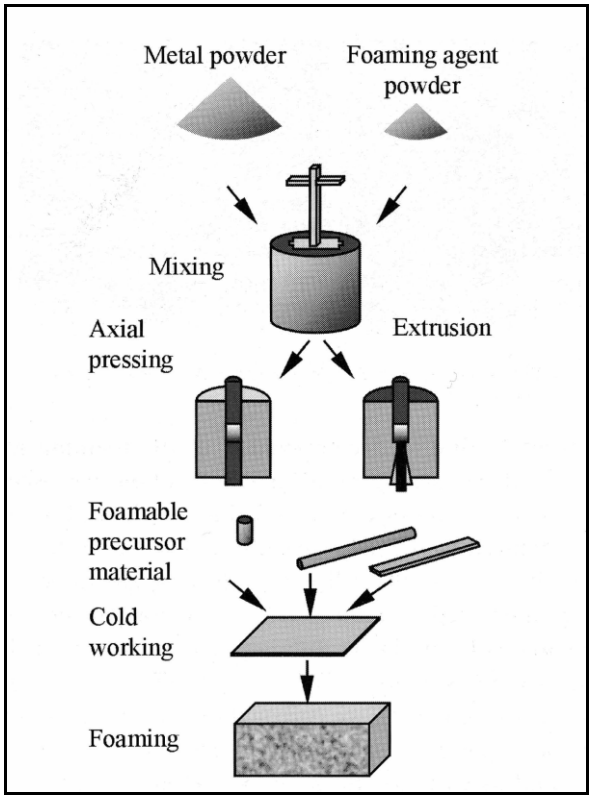

Fig. 1: Powder-metallurgical process (IFAM)

By means of uniaxial compression, extrusion or powder rolling, the available powder mixture is compacted to form a foamable preform. The foaming agent starts to act when the preform is then heated to temperatures above the melting point; the foaming agent decomposes and the released gas forces the material to expand whilst forming a highly porous, closed-cell pore structure. Prior to foaming, the precursor material can be processed to form sheets, rods, profiles, etc. by conventional techniques[7].

Aluminium foams made using the PM process usually exhibit a density of between 0.4 and 1g/cm^3.

Aluminium foam with the brand name ALULIGHT (ALULIGHT International GmbH (SHW/ECKART)) and FOAMINAL (SCHUNK /HONSEL) is available on the market. These aluminium foams are based on a powder-metallurgical process patented by the Fraunhofer Institute in Bremen[1, 2]. This method makes it easy to produce near net-shaped parts[3] by inserting the precursor material into a mould and expanding it by heating.

2.2 Melt-metallurgical Process

Aluminium foam produced from the so-called melt foaming route was developed simultaneously and independently by ALCAN and NORSK HYDRO[6, 7] in the late 1980's and 1990's. ALCAN has now licensed their patent rights to the Canadian company CYMAT[4, 5], who are at present preparing for commercial production. The melt-metallurgical process starts by melting down the aluminium matrix metal (Al-wrought or Al-casting alloys). Depending on the process variant, appropriate refractory particles (e.g. Al2O3 or SiC) are added to the melt between 10 to 30vol%. The particle size lies in general between 10 and 30mm. To form aluminium foam, gas is dispersed into small bubbles in the aluminium composite melt by rotor impellers (Fig.2).

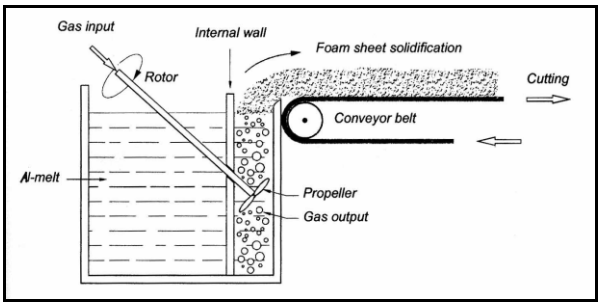

Fig. 2: Melt-metallurgical process (Norsk Hydro)

The walls of the bubbles created are stabilised by the refractory particles added, avoiding coalescence between them. The gas bubbles rise to the surface, where they accumulate. The still liquid aluminium foam is removed from the surface by a conveyor belt and conserved in its porous form through suitable cooling. Foam may be produced in densities from 0.1 to 0.5g/cm^3 by this method. This corresponds to an average pore size of 25 to 3mm. The density is controlled by the process parameters, the most important being the rotor speed, the gas flow through the rotors and the amount of particles added to the melt. Aluminium foam panels can be produced by this method having a thickness of 25 to 150mm, a width of 70 to 150cm and a length of 200cm[7]. This initial semi-finished product can then be processed further.

3 Fatigue Behaviour of Aluminium Foam

In order to be in a position to evaluate future applications of aluminium foam in helicopters (vibrating environment), it is absolutely necessary to gain a fundamental understanding and basic knowledge about the degradation of strength with cyclic loading and about the kind of failures that occur.

Aluminium foam produced from metal powder (AA6061) and aluminium melt (AlSi7Mg+15%SiCp) was fatigue-tested using Wöhler's method. The stress ratio was kept constant during testing (R=-1), and fatigue tests were thus performed under completely reversed stresses (uniaxial: tensile/compressive). The stress amplitude was then varied from one specimen to the next and the test procedure was able to establish the greatest loading endured "infinitely often" ($N \geq 10^7$) without fracture. The number of cycles endured by the test specimens up to fracture was determined under conditions of controlled sinusoidal stress amplitudes while observing the strain response. This data was used to determine the fatigue strength for both types of aluminium foam tested, and S-N curves were calculated using Weibull's method. Hysteresis was also measured for different loadings to provide information on the specific fatigue behaviour of the two types of aluminium foam. Fracture surfaces of representative fatigue-tested specimens were recorded and compared to complete the analysis. The results from these investigations shall be presented and discussed in detail in the following; first, however, let us make some brief remarks regarding the preparation of specimens.

The specimens tested (length: 80mm, cross section: 50x50mm^2) were produced from the aluminium foam material AA6061, manufactured and supplied by IFAM and from AlSi7Mg+15%SiC_p, manufactured and supplied by NORSK HYDRO. The specimens were not subjected to additional heat treatment. Skins and density gradient zones near the surface were removed and the specimen only consisted of the pure foam core. Specimens with cracks, damage to cell walls or foam defects were rejected. Since the specimens were subjected to fatigue testing under completely reversed stresses (uniaxial: tensile

/compressive), it is necessary to bond the specimen to the testing fixtures. A specially adapted bonding device and intermediate fixing plates were therefore used. The bonding surface was also increased by outer bonding elbows. Finally, the effective fatigue- loaded specimen volume amounted to 50x50x50mm3. The intermediate fixing plates and test fixtures were centred during testing and bonding to ensure correct alignment of the test adapters. This procedure was carried out to avoid misalignment due to twisting (rotation of clamps/test fixtures) or displacement of their axes of symmetry[11, 12, 13].

3.1 Powder-metallurgical Aluminium Foam (AA6061)

First of all, some specimens were tested as to tensile and compressive strength. Then, taking these values into account, the remaining specimens were, as described previously, tested as to fatigue resistance. Subsequently, fitted curves to determine the fatigue resistance were computed, applying Weibull's method and the method of the smallest square fits.

The value pairs for voltage amplitude applied and number of load cycles endured as well as the associated Wöhler curve are represented for the PM-based AA6061 foam in Fig. 3. The technically relevant value for the fatigue strength can be given with 0.8MPa.

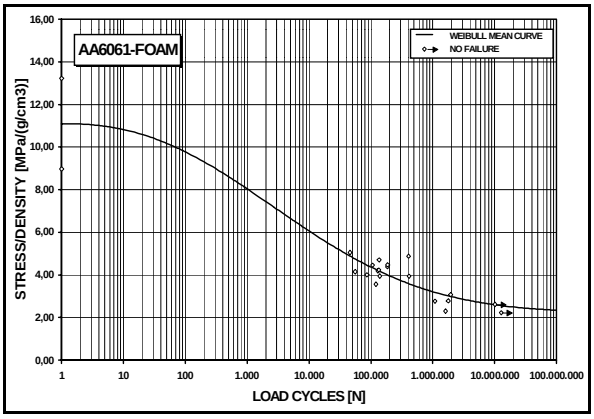

Fig. 3: S-N diagram for AA6061 foam

The mean specific density of the specimens tested was scattered. The degree of scatter amounted to 0.402±0.039g/cm^3. Consequently, the specific strength was plotted in the Wöhler curve versus the number of load cycles endured[9, 10, 11].

The stress-elongation hysteresis comprises fundamental information about the cyclical fatigue behaviour of the foam tested. After all, the elongation measured is composed of a plastic and an elastic share. Hence the hysteresis comprises the entirety of all the processes occurring in the material during fatigue, from the formation of dislocations over their interaction up to crack formation and propagation[8, 10].

The curve of the hysteresis was measured for various cyclical load levels and is illustrated representatively in Fig. 4 for one specimen.

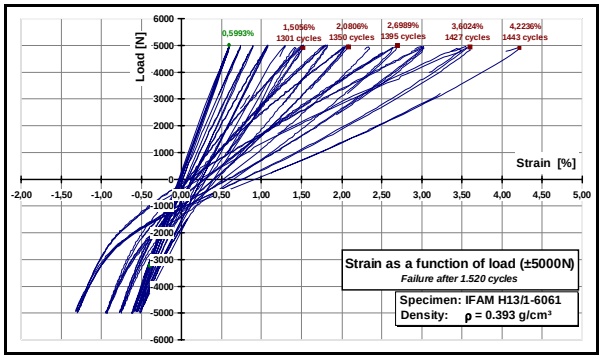

Fig. 4: Stress-strain hysteresis as a function of load cycles for IFAM H13/1-6061

The remaining plastic elongations increase under tensile as well as compressive loading in the course of the fatigue tests. This could be regarded as a de-strengthening of the aluminium foam under dynamic loading. All specimens of this type of foam failed after an accumulated overall plastic elongation of approx. 2.0 to 4.0% was reached. During the tensile test, a tensile strain at break of merely approx. 0.9 to 1.0% was observed. In addition, a drop in Young's modulus is observed as the number of load cycles increases. The cause may be a change in cell geometry due to increasing remaining plastic elongation and possible incipient cracks in the cell walls[8, 10, 12, 13].

Figs. 5 and 6 show the appearance of the pore structure of a PM-based aluminium foam. The specimen shown in Fig. 5 exhibited a relatively homogeneous pore structure in the fracture cross section. The specific fatigue stress applied to this specimen is about 20% higher than for the specimen shown in Fig. 6, but both specimens endured roughly the same cycles to fracture.

As can be seen from Fig. 6, the difference is obviously due to the pronounced inhomogeneity of the cell structure of this specimen; as is to be expected, it is less load-tolerant.

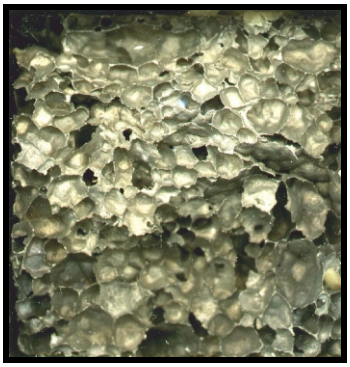

Fig. 5: Fracture Surface
Specimen: IFAM H05/2
Number of cycles: 134,990
Stress/density: 4.23 MPa/(g/cm^3)
Density: 0.378 g/cm^3

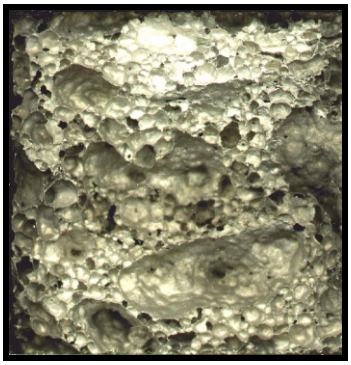

Fig. 6: Fracture Surface
Specimen: IFAM H14/2
Number of cycles: 129,406
Stress/density: 3.56 MPa/(g/cm^3)
Density: 0.393 g/cm^3

3.2 Melt-metallurgical Aluminium Foam (AlSi7Mg+15%SiC$_p$)

As has already been described for the PM-based aluminium foam, some specimens are tested first of all for tensile and compressive strength before commencing the dynamic test with the remaining specimens. In addition, two different extraction directions are studied during the tests on melt-metallurgical aluminium foam, namely perpendicular and parallel to the so-called direction of foam growth.

The experimental results and the fatigue curves calculated are shown in Fig. 7 for the two extraction directions, perpendicular and parallel to the direction of foam growth. The fatigue strength can be determined as being 1 MPa perpendicular to the direction of foam growth and 0.6MPa in the parallel direction[10, 12, 13]. The average aluminium foam density was 0.29±0.027g/cm^3. The fatigue curve for specimens loaded parallel to the direction of foam growth is inferior to the curve for the specimens loaded perpendicular to the direction of foam growth[12, 13].

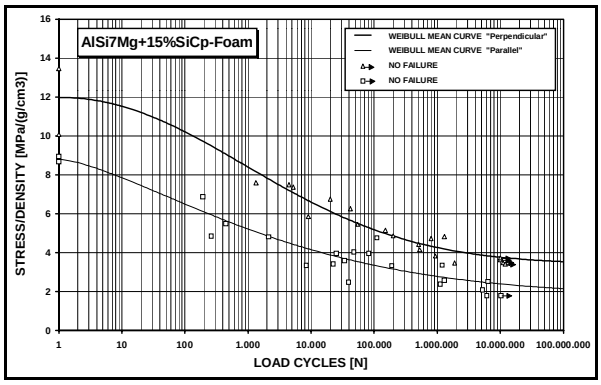

Fig. 7: S-N diagram for AlSi7Mg+15%SiC$_p$ foam-loaded parallel (square) and perpendicular (triangles) to the direction of foam growth.

The difference in fatigue strength for the direction tested might be explained by the density gradient in the direction of foam growth and the anisotropic cell shape, both due to the effect of gravity during manufacturing.

For this type of aluminium foam as well, the progress of hysteresis was measured for different vibration loads to gain an insight into its specific fatigue behaviour[8].

Fig. 8 shows the hysteresis for a specimen tested perpendicular to the foaming direction that failed after 1,299,693 cycles. The residual strain increases considerably under tensile loads and decreases under compressive loads.

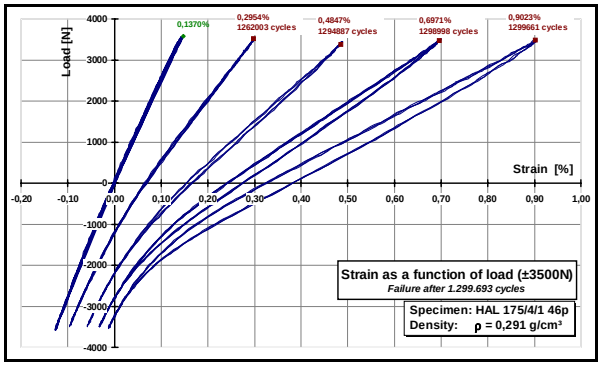

Fig. 8: Stress-strain hysteresis as a function of load cycles for the specimen HAL 175/4/1 46p loaded perpendicular to the direction of foam growth

Comparing Fig. 8 with Fig. 4 shows that, when subjected to tensile loading, the melt-metallurgy-based

aluminium foam evidently responds similarly to the PM-based foam. However, the behaviour of both types of aluminium foam in the area subjected to compressive loading is opposite to each other.

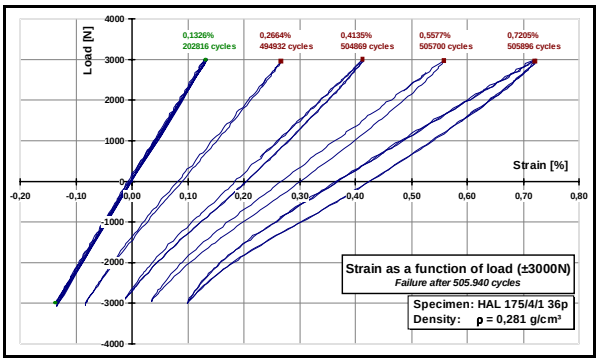

Fig. 9: Stress-strain hysteresis as a function of load cycles for the specimen HAL 175/4/1 36p loaded perpendicular to the direction of foam growth

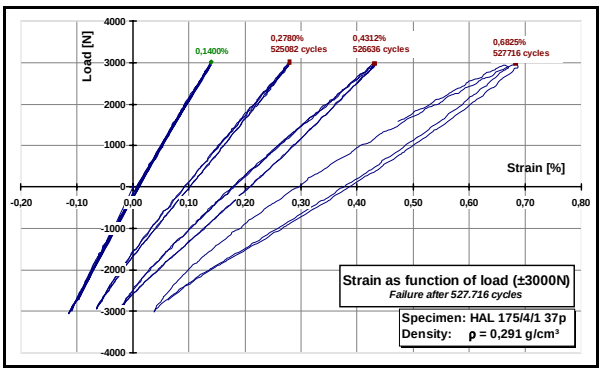

Fig. 10: Stress-strain hysteresis as a function of load cycles for the specimen HAL 175/4/1 37p loaded perpendicular to the direction of foam growth

In Figs. 9 and 10, the curve of the hysteresis of two specimens is shown which, up to ultimate failure due to fracture, have endured roughly the same number of load cycles (approx. 500,000 cycles) with almost the same loading. It can be seen that the curves of both hystereses are almost identical.

Figs. 8, 9 and 10 illustrate very clearly how the hysteresis continues to widen as material fatigue increases, until the specimens finally fail.

The behaviour of the aluminium foam obtained through melt metallurgy is perpendicular to the direction of foam growth in the case of dynamic loading, as described just above, almost identical to the behaviour in the case of dynamic loading parallel to the direction of foam growth. For this reason, examples from the low-cycle fatigue area were chosen for the loads parallel to the direction of foam growth.

Fig. 11 therefore shows very clearly the pronounced widening of the hysteresis that was seen from the very beginning. Consequently, the material is already subject during the first load cycle to such high fatigue that the specimen already fails after approx. 253 load cycles.

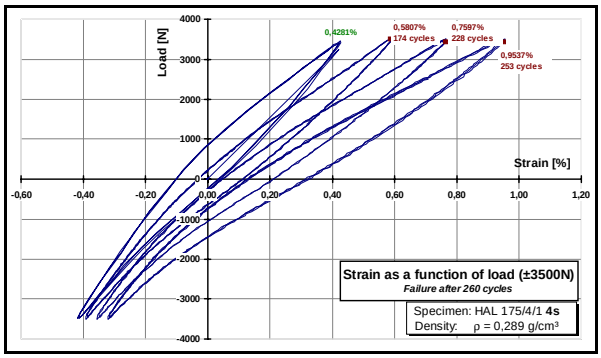

Fig. 11: Stress-strain hysteresis as a function of load cycles for the specimen HAL 175/4/1 4s loaded parallel to the direction of foam growth

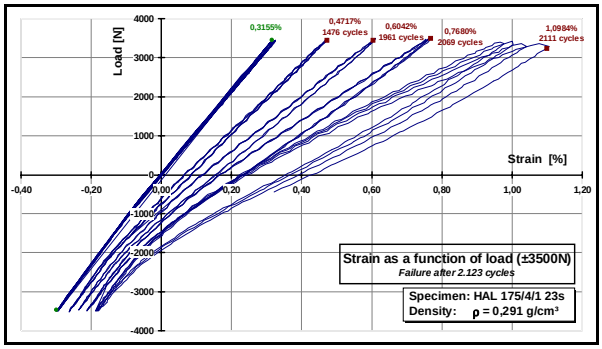

Fig. 12: Stress-strain hysteresis as a function of load cycles for the specimen HAL 175/4/1 23s loaded parallel to the direction of foam growth

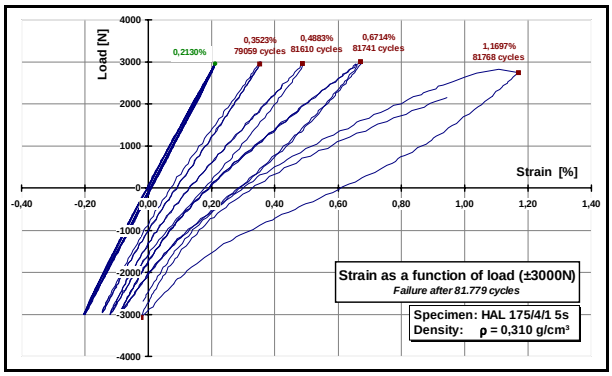

Fig. 13: Stress-strain hysteresis as a function of load cycles for the specimen HAL 175/4/1 5s loaded parallel to the direction of foam growth

Comparing Fig. 12 with Fig. 11 shows that hysteresis spreads far later, even if the specimen from Fig. 12

already failed after approx. 2,111 load cycles. This feature is shared by the specimen from Fig. 13 with its 81,768 load cycles in the course of hysteresis with the specimen from Fig. 12.

To sum up, it can be said that the residual strain increases considerably under tensile loads and decreases under compressive loads. The same phenomenon was observed for specimens tested parallel to the direction of foam growth and perpendicular as well. All specimens failed after accumulating a residual strain of 0.7 to 1.2%. These values appear quite high compared to those of the tensile test (0.2 to 0.5%).

The fracture surfaces from Figs. 14 and 15 reveal the pore structure of melt-metallurgical aluminium foam parallel to the direction of growth.

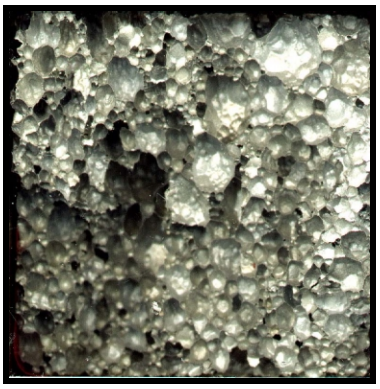

Fig. 14: Fracture Surface
Specimen: HAL 175/4/1 36p
Number of cycles: 505,940
Stress/density: 4.27 MPa/(g/cm^3)
Density: 0.281 g/cm^3

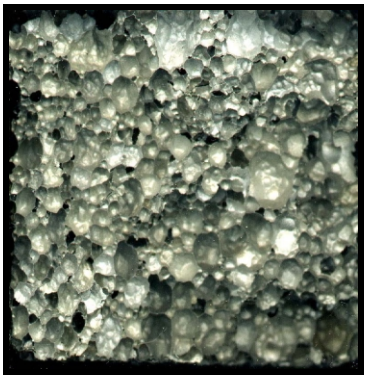

Fig. 15: Fracture Surface
Specimen: HAL 175/4/1 37p
Number of cycles: 526,716
Stress/density: 4.12 MPa/(g/cm^3)
Density: 0.291 g/cm^3

In the case of identical specific loading during the dynamic test, both specimens failed after approximately the same number of load cycles (about 500,000). Both figures reveal that the pore structure is homogeneous to roughly the same extent. The curve of the hysteresis was already very similar for both specimens (Figs. 9 and 10).

Fig. 16: Fracture Surface
Specimen: HAL 175/4/1 16s
Number of cycles: 39,144
Stress/density: 2.45 MPa/(g/cm^3)
Density: 0.326 g/cm^3

Fig. 17: Fracture Surface
Specimen: HAL 175/4/1 22s
Number of cycles: 1,195,475
Stress/density: 3,34 MPa/(g/cm^3)
Density: 0.299 g/cm^3

The extremely weakening effect of a relatively inhomogeneous pore structure is illustrated by means of the two following Figs. 16 and 17. Both figures depict the pore structure of melt-metallurgy-based aluminium foam perpendicular to the direction of foam growth.

Both specimens were subjected to fatigue loads parallel to the direction of foam growth. The specific stress (stress/density) applied to the specimen in Fig.

17 is about 30% greater than that applied to the specimen from Fig. 16.

Nevertheless, the specimen shown in Fig. 17 endured approximately 40 times more cycles to fracture. The homogeneity of the foam structure in the specimen from Fig. 16 is clearly the main reason for its superior fatigue resistance.

Generally, for both types of aluminium foam, it appears that tensile loads are more damaging than compressive loads and that the shape of the cells is being stretched increasingly in the direction of loading as fatigue progresses. Furthermore, it might be assumed that softening of the aluminium foam occurs during fatigue testing. In addition, a significant drop in Young's modulus is observed for the melt-metallurgical as well as the powder-metallurgical aluminium foam. This drop in modulus may be attributed to geometric changes in the cell shape due to strain and the cracking of cell walls. Conspicuous for both types of aluminium foam is that Young's modulus continues to drop under tensile loading as fatigue increases. This may additionally support the assumption that aluminium foam is subject to greater fatigue under tensile loading than under compressive loading[10, 12, 13].

A difference to be pointed out between both types of aluminium foam is that the melt-metallurgical aluminium foam already fails after overall plastic elongation of 0.7 to 1.2% when subjected to dynamic loading, in contrast to 2.0 to 4.0% for the powder-metallurgical foam. Hence, the former is significantly less ductile.

However, the homogeneity of the pore structure is the most important parameter influencing the increase in fatigue of aluminium-foamed specimens and components[10].

4 Demonstrator: Service Step of the EC135 Helicopter[13]

Finally, knowing the properties of aluminium foam, the specific processes as well as the specified requirements for diverse components, the service step of the EC135 (Fig. 18) was selected. The selection of this first demonstrator bore in mind the particular advantage of the powder-metallurgical process, namely near net-shape foaming, with a view to the perhaps resultant potential for cutting production costs.

Fig. 18: Helicopter EC135 with detail showing opened service step

The design and construction of the service step were optimised iteratively in consideration of the manufacturing process, with the aim of fulfilling all requirements of the current series solution neutrally with respect to weight. This led to the concept of a self-supporting, reinforced integral aluminium-foamed body, as shown in Fig. 19. The service step currently used in the series is a relatively complex honeycomb sandwich design (Fig. 20).

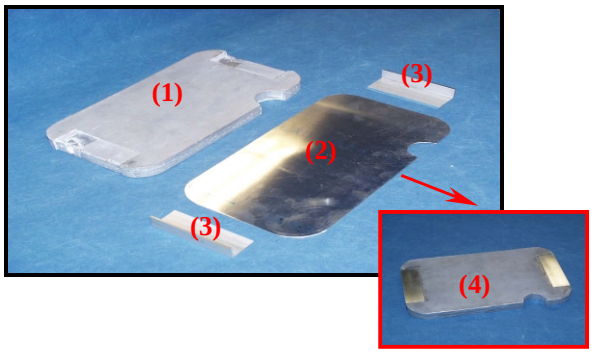

Fig. 19: Service step of integral aluminium foam construction (4) made of an aluminium-foamed body (1), reinforced with two angle sections (3) and a cover plate

The forces introduced are distributed over a large area to the aluminium-foamed body via the angle sections attached laterally to it. The cover plate ensures the so-called damage tolerance of the component. In case the foamed body breaks through, it is held together by the bonding with the cover plate. The simple design is particularly noteworthy.

Finally, the component test verified that the service step of aluminium foam fulfils all the relevant requirements; however, the weight is currently still approx. 20% higher. A positive aspect is that the

manufacturing costs may perhaps be cut by at least 50%.

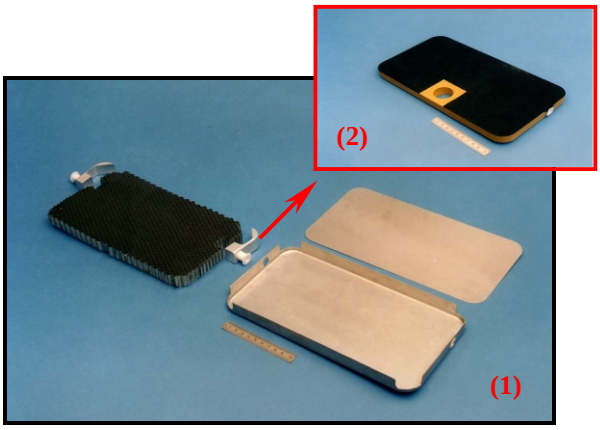

Fig. 20: Service step of honeycomb construction in the initial state (1) and after assembly (2)

In the final instance, the question of quality control naturally arises, especially with regard to preventing nonpermissible inhomogeneities in the pore structure.

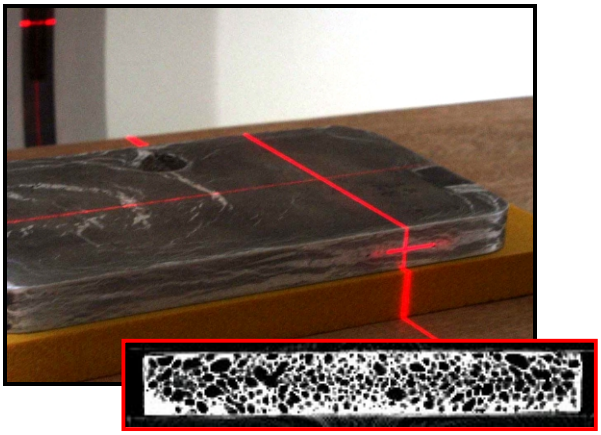
Fig. 21: Non-destructive visualisation of the pore structure by means of computer tomography

Optimal, non-destructive monitoring of the quality of the pore structure can be achieved thanks to computer tomography. A section through an aluminium-foamed body is shown in Fig. 21.

5 Summary

Two different methods for producing aluminium foam were presented – melt metallurgy and powder metallurgy. It should be mentioned in particular that the latter offers the process-specific possibility of near net-shape foaming, which might involve a significant potential for cutting production costs with suitable components.

It could be shown that the specific fatigue strengths (fatigue strength/density) for both types of foaming processes (using metal powder and aluminium melt) lie in the same range.

Despite the relatively small number of specimens tested for each fatigue curve, the fatigue test is sensitive enough to confirm anisotropy in aluminium foam produced from aluminium melt. This means that the fatigue strength perpendicular to the direction of foam is superior to the fatigue strength parallel to the direction of foam growth.

As regards the demonstrator selected – the service step of the EC135 – it can be said that this represents a rather “simpler” component of the secondary structure of the helicopter. But it was particularly suitable for representatively evaluating the applicability of aluminium foam for more complex secondary structural components.

The service step made of aluminium foam offers, in contrast to the currently used honeycomb sandwich construction, the advantages of the more favourable semi-finished product, and in addition fewer single components are needed; further, expensive production steps can be dispensed with completely thanks to the possibility of near net-shape foaming.

To sum up this study, it should be remembered that – as can be said generally of every new material – aluminium foam used in a helicopter can only compete with other light-weight materials if it offers significant cost- and/or weight-related advantages. The latter will be extremely difficult to achieve in view of the already very sophisticated light-weight construction; the former will be easier to achieve, which could also be verified very convincingly in the case of the service step.

Acknowledgements

Special thanks are due to Hydro Aluminium s.a., Sunndalsora, Norway and the Fraunhofer Institut für angewandte Materialforschung (IFAM), Bremen, Germany for the provision of a large number of semi-finished products made of aluminium foam.

The research work has been carried out within the framework of the European Commission's “Industrial and Materials Technologies” multiannual (94-98) programme for R&D. The authors gratefully acknowledge the collaboration of all the partners on the METEOR project “Light-weight Metal Foam

Components for the Transport Industry" (Contract BRPR-CT96-0215, Project BE96-3018).

References

[1] J. Banhart, J. Baumeister, *Production Methods for Metallic Foams*, MRS Symposium Proceeding Vol. 521, San Francisco **1998**, pp. 121-132.

[2] J. Baumeister, *Verfahren zur Herstellung poröser Metallkörper*, German Patent DE 4 018 360 C1, **1991**.

[3] F. Simancik, F. Schörghuber, E. Hartl, *Verfahren zur Herstellung von Formteilen aus Metallschaum*, Austrian patent application, **1996**.

[4] J. T. Woods, *Production and applications of Continously Cast Foamed Aluminium*, Proceedings of the Fraunhofer USA Metal Foam Symposium, Stanton, Delaware, October 7-8, **1997**.

[5] I. Jin, L. D. Kenny, H. Sang, *US Patent No. 5 112 697*, **1992**.

[6] P. Åsholt, *Aluminium Foam Produced by the Melt Foaming Route Process, Properties and Applications* (Eds: J. Banhart, M. F. Ashby, N. A. Fleck), MIT Publishing, Bremen **1999**, pp. 133-140.

[7] C. Körner, R. F. Singer, *Processing of Metal Foams - Challenges and Opportunities*, Adv. Eng. Mat., Vol. 2, No. 4, April **2000**.

[8] ASM Handbook, Vol. 19, *Fatigue and Fracture*, ASM International, **1996**.

[9] W. Weibull, *Fatigue Testing and Analysis of Results*, Pergamon Press, **1961**.

[10] M. F. Ashby, T. Evany, N. A. Fleck, L. J. Gibson, J. W. Hutchinson, H. N. G. Wadley, *Metal Foams: A Design Guide*, Butterworth-Heinemann, Oxford, **2000**.

[11] DIN 50100, Dauerschwingversuch, DIN-Taschenbuch 19, Beuth Verlag, **1996**.

[12] O. Schultz, A. des Ligneris, O. Haider, P. Starke, *Fatigue Behaviour, Strength, and Failure of Aluminium Foam*, Adv. Eng. Mat., Vol. 2, No. 4, April **2000**.

[13] O. Schultz, R. Schindler, *Aluminiumschaum: Dynamische Festigkeit und Anwendung im Hubschrauber*, Symposium Metal Foams 2000, Vienna, Februar **2000**.